Modified red clays as adsorbents in the removal of cationic dyes from aqueous solutions

I. Carazeanu Popovici[a], I. Rosca[a,b], A. Dumbrava[a,*]
[a]*Ovidius University of Constanta, Department of Chemistry and Chemical Engineering, 124 Mamaia Blvd., 900527 Constanta, Romania*
[b]*University Politehnica of Bucharest, Department of Inorganic Chemistry, Physical Chemistry and Electrochemistry, 1-7 Polizu Street, Bucharest 011061, Romania*

Thermal and thermo-chemical modification methods were applied to a red clay mineral and the resulted products were comparatively studied. The modified clays were characterized by XRD, XRF, UV-vis and FTIR spectroscopy. The adsorption properties towards two cationic dyes, namely methylene blue and crystal violet, were investigated and the effect of initial concentration and contact time was analyzed, revealing superior adsorption properties for the thermo-chemical modified clay. The values of dye removal rate are very high, over 85%, with better adsorption of methylene blue and a competition between dyes as demonstrated by using binary solutions. The best match with the experimental results was obtained for the pseudo-second-order kinetic model.

(Received February 15, 2023; Accepted May 2, 2023)

Keywords: Calcined red clay, Starch modified red clay, Cationic dye adsorption, Methylene blue, Crystal violet, Wastewater treatment

1. Introduction

The clays and clay minerals, composed of hydrated aluminosilicates and weathered rocks, are used in increasing quantities in cosmetics, therapeutic and pharmaceutical applications, wine clarification in food industry, etc. [1]. But not least, the naturally occurring clays have received a great research attention in the remediation and retention of contaminants, due some reasons like their wider availability, cheapness, nontoxic nature, and a high capacity to adsorb water [2]. They have also properties like charge density, high surface area, and swelling capacities, which recommend them for a low cost remediation of contaminated aqueous systems and soils [2, 3]. Since the surface of clay minerals is negatively charged and hydrophilic, they serve as very good adsorbents of cationic and hydrophilic contaminants, but do not always perform well for adsorbing anionic and hydrophobic pollutants [2]. A lot of studies involving a large variety of clays utilized as dyes adsorbents in wastewater treatment were published [e.g. 4, 5].

The study of the relationship between clay surface area, size/mesh and adsorption capacity demonstrated that the major reason for the high adsorption capacity of clay materials is their high surface areas, but some exceptions to this general rule were evidenced, being also important in the description of adsorbent quality. Accordingly, the clay morphology, the pore size, the charge density, and also the swelling properties influence the adsorption process [6]. The adsorption capacity can be increased by the physical and chemical modification methods, such as the thermal treatment, acid treatment and intercalation of organic compounds [7, 8].

The thermal treatment (calcination), as a physical treatment technique, has the advantage of being a simple and cheap method [9]. During the heating, the structure and composition as well as the properties of clay minerals are modified, the temperature at which changes occur varying a lot with the clay mineral. The calcination temperature depends on the particle size and on the heating regime, but the impurities in natural clays are also important. It was established that four temperature ranges, in which significant changes occur in the structures of clay minerals, are

* Corresponding author: adumbrava@univ-ovidius.ro
https://doi.org/10.15251/DJNB.2023.182.567

distinguished in the clay calcination process [10, 11]. The intercalation of organic compounds is a modification method based on the incorporation of organic molecules, including polymers, into the interlayer space, with the obtaining of organoclays [9]. To avoid the disadvantages of synthetic polymers, several biodegradable polymers were used in the synthesis of clay-based composites [12]. Biopolymer–clay nanocomposites, a new class of materials with potentially improved properties, are prepared by addition of low amounts of clay to the biopolymer matrix. Potential sources for a wide variety of renewable and ecologically friendly polymers are the plants since starches, the dominant carbohydrate reserve material of higher plants, are abundant and relatively inexpensive biopolymers [13]. Thus, the starch has attracted considerable attention as biopolymer in the synthesis of clay-based nanocomposites, with possible applications in food, medical, cosmetics and healthcare [14].

Various dyes are used in industries like rubber, textiles, cosmetics, plastics, leather, food and paper, and they can be found in wastewaters discharged from these industries. In general, dyes are stable to light, heat and oxidizing agents, being usually non-biodegradable. The dyes give color to the receiving water bodies and, besides the aesthetic aspect, they reduce the penetration of sunlight to benthic organisms and limit the process of photosynthesis. Moreover, some of the dyes and their metabolites can be mutagens and carcinogens, xenobiotic in nature and aerobically recalcitrant to biodegradation. Consequently, the increasing amount of industrial wastewater has needed the development of methods for the dyes removal from wastewaters [6]. The methods as adsorption, coagulation/flocculation, membrane filtration, chemical oxidation and electrochemical treatment are used for the removal of soluble dyes from wastewaters. The adsorption of dyes depends on several factors, involving both the adsorbent and the dye, and the use of clays as adsorbents in the wastewater treatment received an increasing attention as a very attractive method for pollution remediation because of its economical and environmental advantages [15].

The red clays are clays with a reddish or reddish-brown color, due to hematite, goethite, maghemite, and/or amorphous Fe oxides which were formed as the result of dehydration or oxidation of Fe oxyhydroxides. The red clay sediments were discovered in several geographical regions, including the Carpathian Basin, by both exposures and boreholes [16, 17]. The composition of red clays differs depending on the geographical origin; for example, in the bulk red clay samples collected from the NE Hungarian region, the most abundant minerals are quartz and phyllosilicates, the feldspars are minor constituents, while goethite, hematite, and dolomite are accessory phases. Among the clay minerals, smectite (montmorillonite) and illite are dominant, while kaolinite and chlorite are subordinate [17, 18].

In our study, we considered a natural Romanian red clay which, according to our knowledge, has not been investigated until now. The clay mineral was thermal, respective thermo-chemical modified with potato starch. The utilization of the modified clays in the wastewater treatment for the removal of cationic synthetic dyes was studied, and the influence of both dye and clay in the adsorption process was investigated.

2. Experimental

2.1. Materials

The high purity reagents were obtained from Merck (soluble starch (potato starch), $(C_6H_{10}O_5)_n$) and Sigma-Aldrich (methylene blue, crystal violet), being used as received without further purification. Methylene blue (MB; methylthioninium chloride; 3,7-bis(dimethylamino)phenothiazinium chloride; tetramethylthionine chloride) has the chemical formula $C_{16}H_{18}ClN_3S$ and the molar mass 319.85 g/mol. Crystal violet (CV; gentian violet; methyl violet 10B; 4-{bis[4-(dimethylamino)phenyl]methylene}-N,N-dimethyl-2,5-cyclohexadien-1-iminium chloride) has the chemical formula $C_{25}H_{30}ClN_3$ and the molar mass 407.98 g/mol. The red clay mineral was collected from Dobrogea County, Romania.

2.2. Clay processing

Thermal modification. The red clay was crumbed in a mortar of agate, sieved through a 90 μm mesh size sieve, dried at 65 ^{o}C for 3 h and calcined at 850 ^{o}C for 4 h. The sample was denoted Calcined Red Clay, CRC.

Thermochemical modification. 15 g of crumbed red clay were mixed with 300 mL H_2O and magnetically stired for 2 h at 80 ^{o}C. A solution was obtained by dissolving 10 g of starch in 100 mL H_2O, then magnetically stirred for 2 h at 80 ^{o}C, and finally added in the clay suspension. The resulted gel was magnetically stirred for 2 h at 80 ^{o}C, kept at room temperature for 24 h, filtered, washed with distilled water, and dried at 65 ^{o}C for 3 h. The resulted powder was calcined at 850 ^{o}C for 4 h. The sample was denoted Modified Red Clay, MRC.

2.3. Characterization of clays

The clays were investigated by X-ray diffraction (XRD) performed on a Shimadzu 6000 diffractometer with Ni filtered CuKα radiation, λ = 1.5407 nm, in the range of 2θ = 15 - 60°, scan rate of 2°/min and a step of 0.02°. The chemical composition was determined by X-ray fluorescence spectrometry (XRF) on a Philips PW-1660 spectrometer. The UV–visible diffuse reflectance spectra of powders were recorded in the range of 220 – 850 nm, on a Jasco V 550 spectrophotometer with an integrating sphere using MgO as the reference. The FTIR spectra were recorded on Agilent Cary 630 FTIR spectrometer with a ZnSe ATR, in the wavenumber range of 4000 - 650 cm^{-1}.

2.4. Adsorption experiment

The adsorption of MB and CV was studied by adding 0.1 g of clay in 100 mL solution of different concentrations (15, 30, 45 and 60 mg/L). The mixtures were magnetically stirred at room temperature and samples of 2.5 mL were taken periodical, filtered and centrifuged (Biobase Mini-10K microcentrifuge, 10,000 rpm, 15 min). After the clay separation by filtration and centrifugation, the concentration of dye was determined based on the Beer-Lambert law by measuring the absorbance at 664 nm (for MB [19]), respective 585 nm (for CV [20]), with an UV–Vis spectrophotometer (Jasco V 550).

The dye removal rate (DR%) and the adsorption capacity at equilibrium (Q_e, mg/g) were calculated as follows [19, 21-23]:

$$DR\ \% = \frac{C_0 - C_e}{C_0}\ x100 \tag{1}$$

$$Q_e = (C_0 - C_e)\frac{V}{m} \tag{2}$$

where C_0 is the initial dye concentration (mg/L), C_e (mg/L) is the equilibrium concentration, V is the volume of the dye solution (L) and m is the mass of adsorbent (g).

2.5. Kinetic and isotherm models

2.5.1. Kinetic models

The pseudo-first-order (PFO) and pseudo-second-order (PSO) kinetic models were used for the interaction between the dyes and clay surface as follows [24]:

$$Q_{tPFO} = Q_e(1 - e^{-k_1 t}) \tag{3}$$

$$Q_{tPSO} = \frac{k_2 \cdot Q_e^2 \cdot t}{1 + k_2 \cdot Q_e \cdot t} \tag{4}$$

The linear forms of Equations 3 and 4 are [21, 25]:

$$\ln(Q_e - Q_{tPFO}) = lnQ_e - k_1 \cdot t \tag{5}$$

$$\frac{t}{Q_{tPSO}} = \frac{1}{k_2 \cdot Q_e^2} + \frac{t}{Q_e} \tag{6}$$

where: t (min) is the contact time; k_1 and k_2 are the pseudo-first-order (min^{-1}), respective pseudo-second-order (g/mg·min) adsorption rate constants; Q_e and Q_t are the adsorption capacity (mg/g) at equilibrium and t min, respectively.

2.5.2. Isotherm models

The adsorption isotherms can describe and predict the amount of adsorbed dye as a function of concentration at a constant temperature. The Langmuir and Freundlich models were applied in the study of MB and CV adsorption onto clays [21, 26].

Langmuir isotherm is an empirical model which assumes a monolayer adsorption of the molecules and its linear form is represented as follows [21, 27]:

$$Q_e = Q_{max} - \frac{Q_e}{K_L C_e} \tag{7}$$

$$\frac{1}{Q_e} = \frac{1}{Q_{max}} + \frac{1}{K_L Q_{max} C_e} \tag{8}$$

where Q_e = adsorption quantity of dye on the clay (mg/g), Q_{max} = maximum adsorption amount (mg/g), K_L = Langmuir adsorption equilibrium constant related to the free energy of adsorption (L/mg).

The separation factor (R_L) is a dimensionless constant which indicates if the adsorption process is favorable, being considered an essential characteristics of the Langmuir isotherm [28, 29]:

$$R_L = \frac{1}{1 + K_L \cdot C_0} \tag{9}$$

Based on the R_L values, the adsorption process can be favorable ($0 < R_L < 1$), linear ($R_L = 1$), unfavorable ($R_L > 1$) or irreversible ($R_L = 0$) [28].

Freundlich adsorption isotherm model is not restricted to the monolayer formation and can be applied to the multilayer adsorption. The Freundlich isotherm equation, in a linear form, can be represented as [21, 26, 27]:

$$logQ_e = logK_F + {}^{1}/_{n_F} logC_e \tag{10}$$

where: Q_e = equilibrium adsorption quantity (mg/g), K_F = adsorption capacity (mg/g), n_F = adsorption intensity. A value of n between 2 and 10 means that adsorption occurs readily, while a value less than 0.5 means that the occurrence of adsorption is more difficult [21].

3. Results and discussion

3.1. Characterization of clays

The composition of clays was determined by XRF spectrometry (Table 1).

Table 1. Chemical composition of clays.

Component	Weight (%)	
	CRC	**MRC**
SiO_2	54.48	55.67
Al_2O_3	17.52	19.35
Fe_2O_3	7.76	7.81
CaO	0.72	0.82
MgO	2.76	2.56
$Na_2O + K_2O$	4.92	5.12
Calcination loss	11.84	8.67
Total	**100**	**100**

As can be seen in the Table 1, the presence of iron justifies the clay's designation as "red clay". The metal oxides percentages are almost equal in the thermal and thermo-chemical modified clays, but the calcination loss is lower for MRC. The obtaining of MRC involves the mixing of the red clay mineral with water, implying the lost of water-soluble components, which may be an explanation for differences between the chemical compositions of clays. The presence of residues from the calcination of clay-starch composite precursor, obtained in the first stage of MRC synthesis, can be another explanation for chemical composition of MRC.

X-ray diffraction. The structure of clays was determined by XRD (Fig. 1). The mineralogical composition reveals the presence of muscovite (common mica), low carnegieite, albite, and quartz.

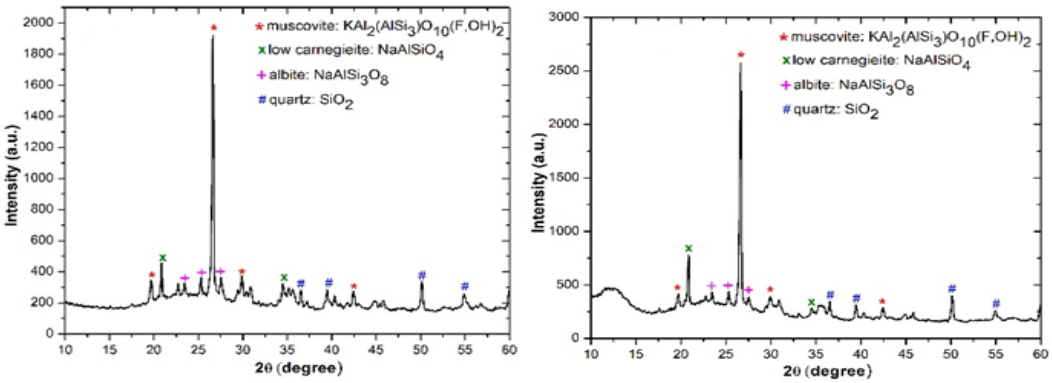

Fig. 1. XRD patterns of CRC (left) and MRC (right).

In addition to the mineralogical composition indicated by XRD, the presence of iron can be explained by its existence as oxides in amorphous forms [16]. In other red clays it was demonstrated the presence of Fe(II) in the structure of muscovite crystal lattice, together with Fe(III) as hematite [30]. Therefore, a distribution of iron in one or more forms, making amorphous compounds and/or in low quantities, which were not identified by XRD, is possible. The low quantity of Mg(II) and Ca(II) is the explanation for their absence from the mineralogical composition. An interesting feature of the XRD pattern of MRC is the presence of a board peak at low values of the diffraction angle (around 12^o). The peak can be assigned to the starch in amorphous form modified by calcination process. The products of starch thermal degradation can be different forms of carbon, considering that the starch molecules were adsorbed in the clay and an insufficient quantity of oxygen was accessible in the thermal degradation.

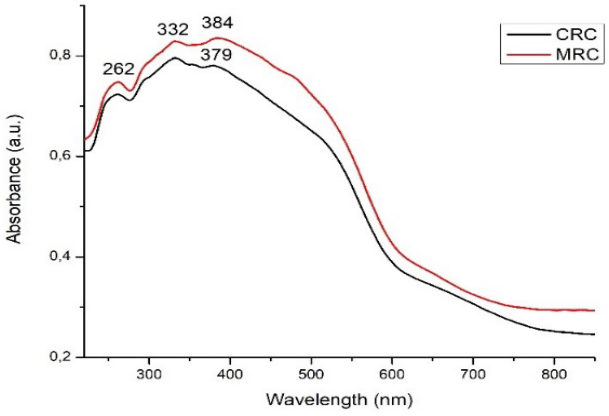

Fig. 2. UV-vis spectra of clays.

UV-vis spectra. Although a multitude of transition metals in trace amounts can be found in the clay minerals, the light absorption in UV-vis domain is almost due to the electronic transitions

which involve iron, being identified absorption bands assigned both to *d-d* and charge transfer transitions [31].

A very intense and broad band centered around 380 nm can be observed in UV-vis spectra of both clays (Fig. 2). Two other peaks and a shoulder are present in each spectrum, in UV domain. The transitions of electrons in UV, involving high energy, are mainly explained by charge-transfer. In the visible domain, two shoulders (around 500, respective 650 nm) can be observed in both spectra, most probable being assigned to *d-d* transitions in iron ions [31]. A more accurate assignment is uncertain in the absence of more precise information related to the oxidation state and coordination of Fe ions. Moreover, a similar shape of both spectra can be observed, with a prominence of shoulders in visible for MRC.

FTIR spectra. Generally, the FTIR spectra of clays are dominated by a very strong band, assigned to the Si–O stretching vibrations, situated around 1000 cm^{-1} [32]. In the FTIR spectra of studied clays (Fig. 3) a very strong band, situated at about 1010 cm^{-1} (1006, respective 1014 cm^{-1}) can be observed; it is assigned to antisymmetric stretching of Si-O-Si bridging groups (ν_{as} [Si-O-Si]). In the intermediate frequency range (800-650 cm^{-1}), two bands with medium strength at 775 and 693 cm^{-1} can be also assigned to Si-O-Si vibrations [33].

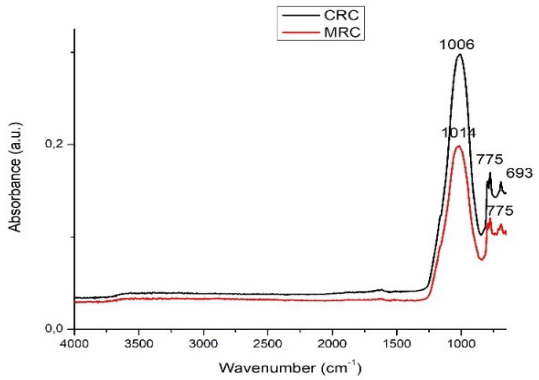

Fig. 3. FTIR spectra of clays.

3.2. Adsorption properties

We tested the thermal, respective thermochemical modified red clay as dyes adsorbent for decontamination of wastewaters. The adsorption of two organic dyes with cationic structure, i.e. methylene blue (MB) and crystal violet (CV) (Fig. 4) was investigated.

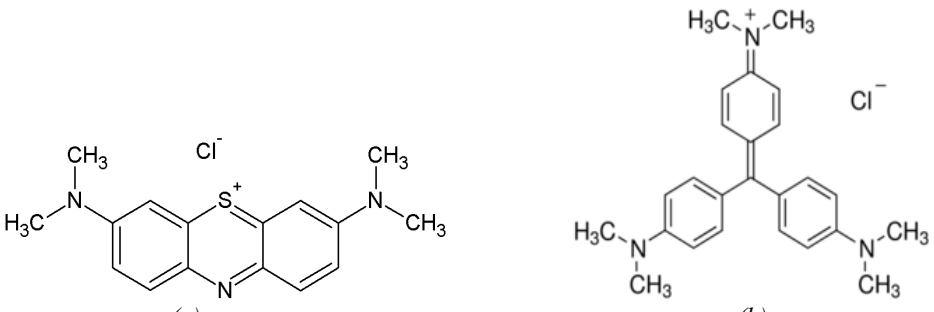

Fig. 4. Chemical structure of dyes: a. methylene blue; b. crystal violet.

The cationic dyes have the same electric charge, but different chemical structure, namely MB has a linear structure while CV has a trigonal planar one. Different concentrations of MB and CV solutions (15, 30, 45 and 60 mg/L) and also a mixed solution of MB and CV (15 mg/L MB and 15 mg/L CV) were tested.

The adsorption experiments were carried out for 240 min, when it was considered that the system reached equilibrium. The adsorption properties of clays were estimated by the dye removal

rate (DR%; Eq. 1) and the adsorption capacity (Qe, mg/g; Eq. 2) at equilibrium (Fig. 5). The adsorption capacity was also estimated in mmol/g (Fig. 5.b).

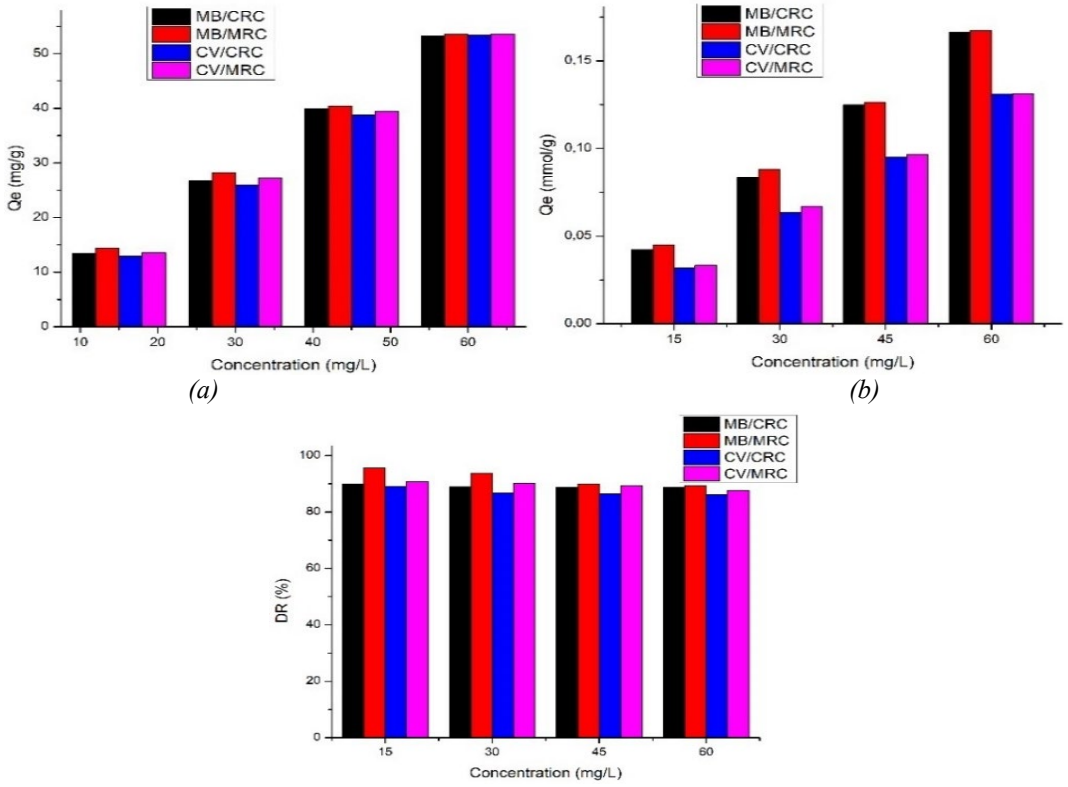

Fig. 5. The adsorption capacity, Q_e, in mg/g (a), respective in mmol/g (b), and the dye removal by adsorption, DR% (c) (t = 240 min).

It can be seen in Fig. 5 that the adsorption capacity strongly increased with the dye concentration, as it was to be expected. By comparing the dyes, a higher adsorption capacity was determined for MB; since the molar mass of MB is lower compared to CV, a higher number of MB mols was adsorbed on the clays' surface. As well, the adsorption capacity of MRC is higher in comparison with CRC.

The values of DR are very high, over 85%, and are decreasing with the dye concentration increasing. The highest DR values were determined for MB in comparison with CV, respective for MRC in comparison with CRC.

In order to examine the clay selectivity in the dyes' adsorption, a binary solution consisting in 15 mg/L MB and 15 mg/L CV was used. The variation of DR with contact time (Fig. 6.a) demonstrated that the dyes are co-adsorbed, MB being adsorbed in a higher quantity both onto CRC and MRC. In comparison with the dyes' adsorption from a single dye solution (Fig. 6.b), a lower quantity of each dye was adsorbed from the binary solution, which may indicate that both dyes are bound to the same sites, being a competition between them. The more favorable adsorption of MB can be corelated with its linear structure and smaller molecule, which can ensure a better adsorption on the clay surface.

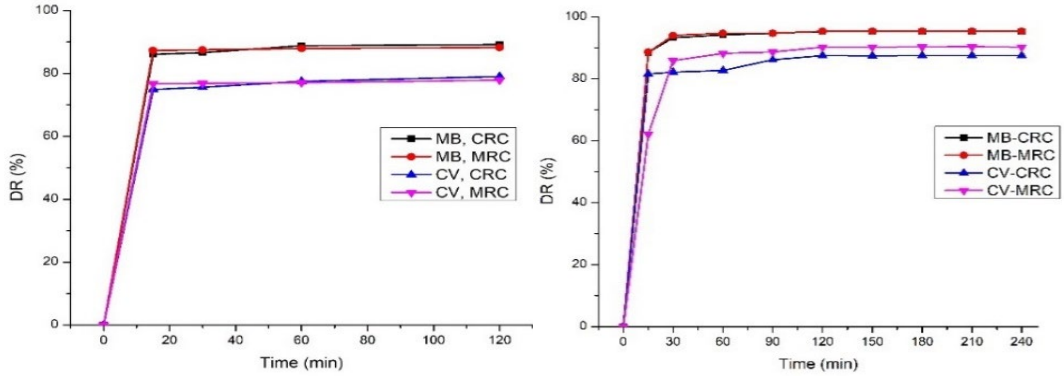

(a) *(b)*

Fig. 6. The variation in time of dye removal (DR%) by adsorption onto CRC and MRC, using a binary solution of MB and CV (a), respective MB and CV solutions of 15 mg/L (b).

Adsorption kinetics and isotherms. The adsorption kinetics were utilized to study the adsorption mechanism. The adsorption of MB and CV onto clays was fitted by pseudo-first-order and pseudo-second-order models (Equations 3-6). The parameters of kinetic models, in comparison with experimental values, are presented in Table 1.

Table 1. Parameters of kinetic models.

Dye - clay	Kinetic model	Parameters	Concentration (mg/L)		
			C_0 = 30	C_0 = 45	C_0 = 60
MB - CRC	Pseudo-first-order (PFO)	Qe, exp. (mg/g)	27.2852	41.3647	54.6671
		Qe, calc. (mg/g)	1.3403	1.5787	2.1893
		k_1 (min^{-1})	0.0078	0.0046	0.0077
		R^2	0.9102	0.9284	0.8774
	Pseudo-second-order (PSO)	Qe, exp. (mg/g)	27.2852	41.3647	54.6671
		Qe, calc. (mg/g)	27.3224	41.3223	54.6448
		k_2 (mg/g·min)	0.0676	0.0152	0.0124
		R^2	0.9999	0.9998	0.9999
MB - MRC	Pseudo-first-order (PFO)	Qe, exp. (mg/g)	28.1318	41.9446	55.5038
		Qe, calc. (mg/g)	1.5360	1.8904	2.6177
		k_1 (min^{-1})	0.0078	0.0098	0.0083
		R^2	0.9747	0.9045	0.9876
	Pseudo- second -order (PSO)	Qe, exp. (mg/g)	28.1318	41.9446	55.5038
		Qe, calc. (mg/g)	28.1690	42.0168	55.5555
		k_2 (mg/g·min)	0.0189	0.0173	0.0113
		R^2	0.9999	0.9999	0.9999
CV - CRC	Pseudo-first-order (PFO)	Qe, exp. (mg/g)	26.7074	40.0836	54.8854
		Qe, calc. (mg/g)	2.0071	1.7577	3.1412
		k_1 (min^{-1})	0.0105	0.0126	0.0081
		R^2	0.9458	0.9042	0.9573
	Pseudo- second -order (PSO)	Qe, exp. (mg/g)	26.7074	40.0836	54.8854
		Qe, calc. (mg/g)	26.8096	40.1606	54.9450
		k_2 (mg/g·min)	0.0155	0.0201	0.0094
		R^2	0.9998	1.0000	0.9999
CV - MRC	Pseudo-first-order (PFO)	Qe, exp. (mg/g)	26.5410	39.4365	53.6122
		Qe, calc. (mg/g)	2.2993	1.4404	8.8075
		k_1 (min^{-1})	0.0131	0.0079	0.0307
		R^2	0.9653	0.965	0.9128
	Pseudo- second -order (PSO)	Qe, exp. (mg/g)	26.5410	39.4365	53.6122
		Qe, calc. (mg/g)	26.7380	39.5257	54.0540
		k_2 (mg/g·min)	0.0137	0.0203	0.0094
		R^2	1.0000	0.9999	1.0000

As can be seen in Table 2 and Fig. 7, the dyes adsorption onto modified clays fitted well with pseudo-second-order kinetic model. It is expected that during the adsorption process the dyes molecules are transferred from solution to the clay surface and then are spread into the pores, the rate-limiting step being the chemical adsorption process in which are involved the clay and dye molecules. The same behavior was observed for other dye-clay systems [33].

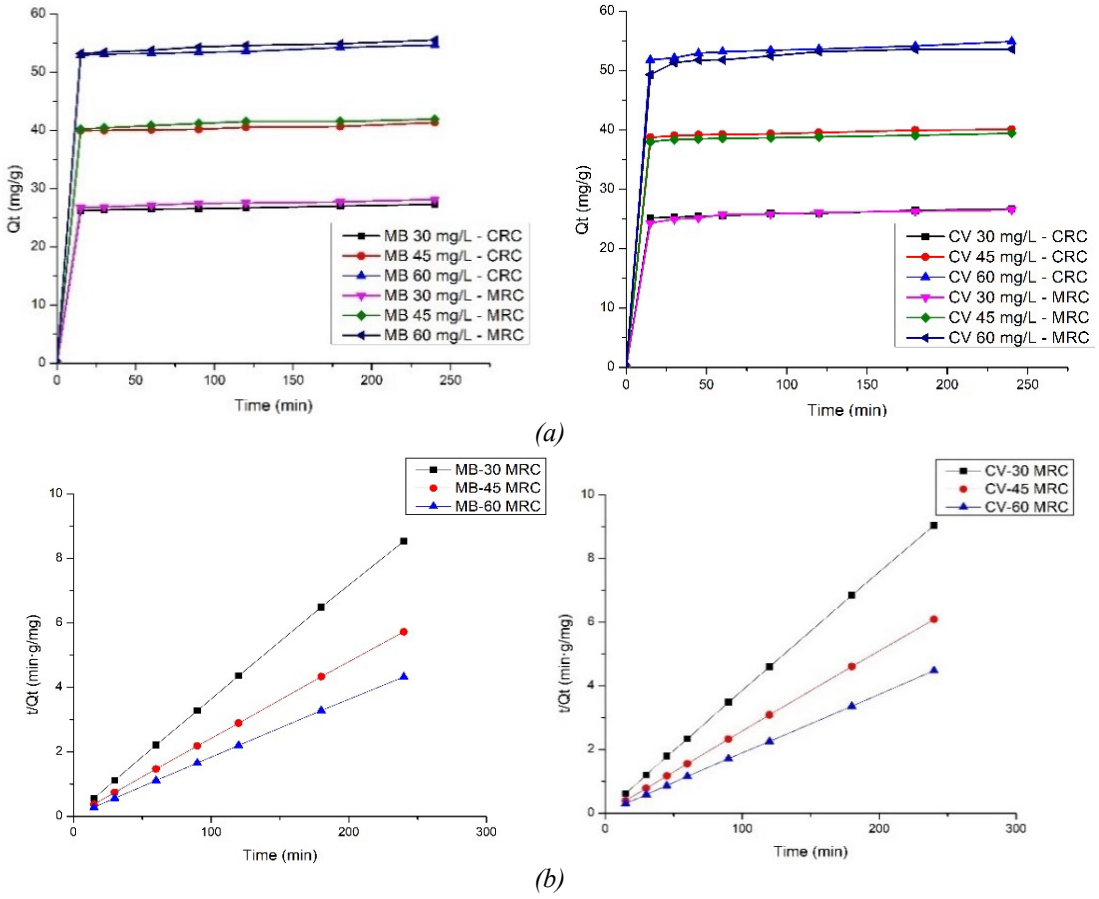

Fig. 7. Kinetic studies of MB and CV uptake by CRC and MRC: effect of contact time (a); pseudo-second order model for adsorption onto MRC (b).

The adsorption behavior was investigated by using Langmuir and Freundlich isotherm models. Therefore, the adsorption equilibrium measurements were used to determine the maximum adsorption capacity in both Langmuir and Freundlich models, adsorption equilibrium constant and separation factor (Langmuir model), and adsorption intensity (Freundlich model).

Table 2. Characteristics of the Langmuir and Freundlich isotherms for MB and CV removal using modified red clays.

Isotherm	**Dye - clay**	Q_{max} **(mg/g)**	K_L **(L/mg)**	R_L	K_F **(mg/g)**	n	R^2
Langmuir	MB - CRC	142.857	0.0570	0.226-0.369	-	-	0.9929
	MB - MRC	181.818	0.0980	0.145-0.254	-	-	1.0000
	CV - CRC	105.263	0.0612	0.214-0.352	-	-	0.9200
	CV - MRC	161.290	0.0620	0.212-0.350	-	-	0.9896
Freundlich	MB - CRC	-	-	-	8.6776	0.8776	0.9876
	MB - MRC	-	-	-	19.1029	1.4349	0.9969
	CV - CRC	-	-	-	4.9865	0.7170	0.9707
	CV - MRC	-	-	-	9.3951	1.1333	0.9796

Based on the correlation coefficients, as they are summarized in Table 2, MB adsorption showed a good fit both with Langmuir and Freundlich isotherms, with slightly higher values for Langmuir model. This means that MB molecules are preferentially adsorbed as monolayer without any interaction with adjacent adsorbed molecules (Langmuir isotherm), but a multilayer adsorption is also favorable. For CV adsorption, a better fit was identified with Langmuir model by using MRC as adsorbent, respective for Freundlich model for adsorption onto CRC. A much lower adsorption capacity was determined for the multilayer model. The results are in concordance with previous studies which identified both monolayer and multilayer adsorption model for the dyes adsorption onto clays. The obtained R_L values between 0 and 1 (i.e. 0.145 – 0.369 for MB, respective 0.212-0.352 for CV) indicate a favorable adsorption. The calculated Q_{max} values follow the same variation as for the experimental values, that is the quantity of adsorbed MB is higher than CV and the MRC clay has a higher adsorption capacity compared to CRC. A similar variation can be noticed for K_F, the higher value being calculated for the adsorption of MB onto MRC. The much lower values of adsorption capacity calculated in Freundlich model in comparison with the experimental values revealed that the multilayer adsorption occurs together with monolayer adsorption. The values of n calculated in Freundlich model are superior to 0.5, indicating that the adsorption is possible, and the highest value was determined for the adsorption of MB onto CRC.

4. Conclusions

In our study we tested two modified clays, obtained by thermal, respective thermo-chemical modification of a red clay mineral which originates from Dobrogea County, Romania. The mineralogical composition of clays consists in muscovite, low carnegieite, albite, and quartz. The difference between chemical composition of clays involves the presence of an amorphous material, obtained by calcination of clay-starch precursor, probably based on activated carbon resulted due to the incomplete calcination of starch. The presence of this material can be an explanation for the better adsorption properties which were observed for MRC in comparison with CRC in the interaction with MB and CV dyes.

The differences between the absorption of MB and CV are due to their structure, the MB molecules, with a lower mass and a linear structure, being preferentially adsorbed into both clays. The kinetic study revealed the adsorption of dyes as a pseudo-second-order process, irrespective of dye and clay. The adsorption study demonstrated that both a monolayer and multilayer adsorption processes are favorable. The study indicated the red clay mineral as a convenient precursor for the obtaining of modified clays, with good adsorbent properties and possible application in wastewater treatment.

References

[1] A.M. Awad, S.M.R. Shaikh, R. Jalab, M.H. Gulied, M.S. Nasser, A. Benamor, S. Adham, Sep. Purif. Technol. 228, 115719 (2019); https://doi.org/10.1016/j.seppur.2019.115719

[2] B. Sarkar, R. Rusmin, U.C. Ugochukwu, R. Mukhopadhyay, K.M. Manjaiah, Modified Clay and Zeolite Nanocomposite Materials" 2019, pp. 113-127; https://doi.org/10.1016/B978-0-12-814617-0.00003-7

[3] S.C.A. Mana, M.M. Hanafiah, A.J.K. Chowdhury, Geol. Ecol. Landsc. 1, 155-161 (2017); https://doi.org/10.1080/24749508.2017.1361128

[4] A. Kausar, M. Iqbal, A. Javed, K. Aftab, Z. Nazli, H.N. Bhatti, S. Nouren, J. Mol. Liq. 256, 395-407 (2018); https://doi.org/10.1016/j.molliq.2018.02.034

[5] A.A. Adeyemo, I.O. Adeoye, O.S. Bello, Appl. Water Sci. 7, 543-568 (2017); https://doi.org/10.1007/s13201-015-0322-y

[6] T. Ngulube, J.R. Gumbo, V. Masindi, A. Maity, J. Environ. Manag. 191, 35-57 (2017); https://doi.org/10.1016/j.jenvman.2016.12.031

[7] S. Barakan, V. Aghazadeh, Environ. Sci. Pollut. Res. 28, 2572-2599 (2021); https://doi.org/10.1007/s11356-020-10985-9

[8] J.A. Cecilia, C. Garcıa-Sancho, E. Vilarrasa-Garcıa, J. Jimenez-Jimenez, E. Rodriguez-Castellon, Chem. Rec. 18, 1085-1104 (2018); https://doi.org/10.1002/tcr.201700107

[9] C. Vasiliki Lazaratou, I.E. Triantaphyllidou, I. Pantelidis, D.A. Chalkias, G. Kakogiannis, D.V. Vayenas, D. Papoulis, Environ. Sci. Pollut. Res. 29, 17737-17756 (2022); https://doi.org/10.1007/s11356-021-17107-z

[10]. L. Heller-Kallai, Clay Science 1, 289-308 (2006); https://doi.org/10.1016/S1572-4352(05)01009-3

[11] L. Heller-Kallai, Developments in Clay Science 5, 411-433 (2013); https://doi.org/10.1016/B978-0-08-098258-8.00014-6

[12] D.R. Paul, L.M. Robeson, Polymer 49, 3187-3204 (2008); https://doi.org/10.1016/j.polymer.2008.04.017

[13]. Y.L. Chung, S. Ansari, L. Estevez, S. Hayrapetyan, E.P. Giannelis, H.M. Lai, Carbohydr. Polym. 79, 391-396 (2010); https://doi.org/10.1016/j.carbpol.2009.08.021

[14] B. Chen, J.R.G. Evans, Carbohydr. Polym. 61, 455-463 (2005); https://doi.org/10.1016/j.carbpol.2005.06.020

[15]. A. Khenifi, Z. Bouberka, F. Sekrane, M. Kameche, Z. Derriche, Adsorption 13, 149-158 (2007); https://doi.org/10.1007/s10450-007-9016-6

[16]. A. Hein, P.M. Day, M.A. Cau Ontiveros, V. Kilikoglou, Appl. Clay Sci. 24, 245- 255 (2004); https://doi.org/10.1016/j.clay.2003.07.009

[17] J. Kovács, B. Raucsik, A. Varga, G. Újvári, G. Varga, F. Ottner, Turkish J. Earth Sci. 22, 414-426 (2013); https://doi.org/10.3906/yer-1201-4

[18] M.I. Khan, Mater. Res. Express 7, 055507 (2020); https://doi.org/10.1088/2053-1591/ab903c

[19] C.A.P. Almeida, N.A. Debacher, A.J. Downs, L. Cottet, C.A.D. Mello, J. Colloid Interface Sci. 332, 46-53 (2009); https://doi.org/10.1016/j.jcis.2008.12.012

[20] Y. Lin, X. He, G. Han, Q. Tian, W. Hu, J. Environ. Sci. 23, 2055-2062 (2011); https://doi.org/10.1016/S1001-0742(10)60643-2

[21] P. Jia, H. Tan, K. Liu, W. Gao, Appl. Sci. 8, 1903 (2018); https://doi.org/10.3390/app8101903

[22] C.H. Weng, Y.F. Pan, J. Hazard. Mater. 144, 355-362 (2007); https://doi.org/10.1016/j.jhazmat.2006.09.097

[23] A.H. Jawada, A.S. Abdulhameed, Surf. Interfaces 18, 100422 (2020); https://doi.org/10.1016/j.surfin.2019.100422

[24] J. Veras Fernandes, A. Mendes Rodrigues, R. Rodrigues Menezes, G. de Araújo Neves, Materials 13, 3600 (2020); https://doi.org/10.3390/ma13163600

[25] H. Demirtas, S. Tasar, F. Kaya, A. Ozer, J. Environ. Chem. Eng. 10, 108062 (2022); https://doi.org/10.1016/j.jece.2022.108062

[26] M.M. Majd, V. Kordzadeh-Kermani, V. Ghalandari, A. Askari, M. Sillanpää, Sci. Total Environ. 812, 151334 (2022); https://doi.org/10.1016/j.scitotenv.2021.151334

[27] M.A. Al-Ghouti, D.A. Da'ana, J. Hazard. Mater. 393, 122383 (2020); https://doi.org/10.1016/j.jhazmat.2020.122383

[28] R.T. Thomas, N. Sandhyarani, RSC Adv. 5, 72683-72690 (2015); https://doi.org/10.1039/C5RA14547C

[29] E. Ajenifuja, J.A. Ajao, E.O.B. Ajayi, Appl. Water. Sci. 7, 2279-2286 (2017); https://doi.org/10.1007/s13201-016-0403-6

[30] V. Valanciene, R. Siauciunas, J. Baltusnikaite, J. Eur. Ceram. Soc. 30, 1609-1617 (2010); https://doi.org/10.1016/j.jeurceramsoc.2010.01.017

[31] S.W. Karickhoff, G.W. Bailey, Clays Clay Miner. 21, 59-70 (1973); https://doi.org/10.1346/CCMN.1973.0210109

[32] J. Madejova, Vib. Spectrosc. 31, 1-10 (2003); https://doi.org/10.1016/S0924-2031(02)00065-6
[33] W.R. Taylor, Proc. Indian Natl. Sci. Acad. 99, 99-117 (1990); https://doi.org/10.1007/BF02871899
[34] E.A. Mohamed, A.Q. Selim, A.M. Zayed, S. Komarneni, M. Mobarak, M.K. Seliem, J. Colloid Interface Sci. 534, 408-419 (2019); https://doi.org/10.1016/j.jcis.2018.09.024